

# Multi-neutron emission of Cd isotopes

A. P. Severyukhin,<sup>1,2</sup> N. N. Arsenyev,<sup>1</sup> I. N. Borzov,<sup>3,1</sup> and E. O. Sushenok<sup>1,2</sup>

<sup>1</sup>*Bogoliubov Laboratory of Theoretical Physics, Joint Institute for Nuclear Research, 141980 Dubna, Moscow region, Russia*

<sup>2</sup>*Dubna State University, Universitetskaya street 19, 141982 Dubna, Moscow region, Russia*

<sup>3</sup>*National Research Centre "Kurchatov Institute", 123182 Moscow, Russia*

(Dated: June 20, 2022)

An influence of the phonon-phonon coupling (PPC) on the  $\beta$ -decay half-lives and multi-neutron emission probabilities is analysed within the microscopic model based on the Skyrme interaction with tensor components included. The finite-rank separable approximation is used in order to handle large two-quasiparticle spaces. The even-even nuclei near the  $r$ -process pathes at  $N = 82$  are studied. The characteristics of ground states,  $2^+$  excitations and  $\beta$ -decay strength of the neutron-rich Cd isotopes are treated in detail. It is shown that a strong redistribution of the Gamow-Teller strength due to the PPC is mostly sensitive to the multi-neutron emission probability of the Cd isotopes.

PACS numbers: 21.60.Jz, 23.40.-s, 21.10.-k, 27.60.+j

## I. INTRODUCTION

The  $\beta$ -decay properties are very important for understanding the nuclear structure evolution at extreme  $N/Z$  ratios, for analysis of the radioactive ion-beam experiments and modeling of astrophysical  $r$ -process [1]. In the last years a renewed attention has been attracted to the delayed multi-neutron emission ( $\beta xn$ ) with  $x = 2, 3, \dots$ . The  $\beta 2n$  emission has been predicted in early 60-s [2] and later observed in for the cases of  $^{11}\text{Li}$  [3] and  $^{30-32}\text{Na}$  [4]. It has also been considered for heavier nuclei in Ref. [5] emphasizing a competition between the sequential and resonant ("di-neutron") emission. Observation of the di-neutron emission in  $^{16}\text{Be}$  decay has been recently claimed [6] (see comment in [7] and discussion in [8]). Now a days Bi isotopes in the mass region  $N > 126$  are the heaviest nuclei where the delayed neutron emission has been studied [9].

A study of  $\beta xn$  processes facilitates developing a self-consistent approach based on the energy density functional (EDF). The process probability depends, first on specific energy "landmarks": the  $\beta$ -decay energy release  $Q_\beta$  and neutron emission thresholds  $S_{xn}$ . An adequate description of these differential quantities poses constraints on the EDF at high isospin-asymmetry regime. Second crucial ingredient is the  $\beta$ -strength function: spectral distribution of the  $\beta$ -decay matrix elements within the  $\beta$ -decay window ( $Q_\beta$ ). Assuming an amplification of the intensity distribution by the integral Fermi factor, the most important contributions come from the allowed Gamow-Teller (GT) and high-energy first-forbidden  $\beta$ -decays. Importantly, they should be treated employing the one and the same self-consistent framework [10, 11].

Experimental studies using the multipole decomposition analysis of the (n,p) and (p,n) reactions [12, 13] found substantial GT strength above the GT resonance peak. This solves a longstanding problem of the missing experimental GT strength. Also it helps to overcome the discrepancies between the theoretical predictions using the one-phonon wave-function of the quasi-

particle random phase approximation (QRPA) and the measurements. It has been found necessary to take into account the coupling with more complex configurations in order to shift some strength to higher transition energies in order to comply with the experimental results [14–16]. Using the Skyrme EDF and the RPA, such attempts in the past [17, 18] have allowed one to understand the damping of charge-exchange resonances and their particle decay. The damping of the GT mode has been investigated using the Skyrme-RPA plus particle-vibration coupling [19]. The main difficulty is that complexity of the calculations increases rapidly with the size of the configurational space and one has to work within limited spaces. The separable form of the residual interaction is the practical advantage of the quasiparticle phonon model (QPM) [20] which allows one to perform the calculations in large configurational spaces [15, 20, 21]. The finite rank separable approximation (FRSA) for the QRPA with Skyrme interactions [22, 23] has been invented to describe charge-exchange excitation modes [24, 25].

In the present paper we concentrate on the delayed multi-neutron emission in the region below the neutron-rich doubly-magic nucleus  $^{132}\text{Sn}$ . The  $\beta$ -decay properties of  $r$ -process "waiting-point nuclei"  $^{129}\text{Ag}$ ,  $^{130}\text{Cd}$ , and  $^{131}\text{In}$  have attracted a lot of experimental efforts recently [26–30]. The theoretical analysis has been done within the microscopic-macroscopic finite-range droplet model (FRDM+QRPA) [26, 31], the continuum QRPA approach with the Fayans EDF (DF3+cQRPA) [10, 11, 32, 33]. Recently, the proton-neutron relativistic QRPA (pn-RQRPA) [34] and the finite-amplitude method (FAM) [35] calculations have appeared. In general, the microscopic approaches [11, 34, 35] described the half-lives and total probabilities of the  $\beta xn$  emission better than the global approach [36] commonly used for astrophysical  $r$ -process modeling. Importantly, all the cited papers have used the one-phonon approximation. This may be not enough for adequate reproduction of the fine structure of the GT strength distribution near the neutron thresholds. Such a detailed analysis is feasible in the large-scale shell-model [37] but this approach is

limited by the number of available  $np-nh$  configurations.

In most of the cases, the experimental  $\beta$ -strength function is absent. The combined analysis of integral  $\beta$ -decay characteristics: the half-lives and  $\beta xn$  emission probabilities ( $P_{xn}$ ) helps to reconstruct the  $\beta$ -strength function. A ratio of  $P_{2n}/P_{1n}$  is a sensitive marker of the GT strength distribution in continuum. This carries back the information on the spin-isospin dependent components of the EDF. The main aim of the present paper is to microscopically describe the change of the  $\beta$ -strength function profile caused by the  $2p-2h$  fragmentation and to analyze its impact on the  $\beta$ -decay half-lives and  $\beta xn$ -emission rates in medium-heavy even-even Cd isotopes close to  $N = 82$  closed shell.

This paper is organized as follows. In Sec. II, we apply the FRSA model for studying the impact of the PPC effects on the delayed multi-neutron emission. In Sec. III we describe the important ingredients used in the  $P_{xn}$  calculations and, in particular,  $Q_\beta$ -value, the low-energy  $2^+$  excitations of the parent nucleus, one and two neutron separation energies for the daughter nucleus. We analyze the results of the calculations of  $\beta$ -decay half-lives in Sec. IV A and the prediction of the  $\beta xn$ -emission probabilities in Sec. IV B. Conclusions are finally drawn in Sec. VI.

## II. $\beta$ -DECAY CHARACTERISTICS WITHIN THE FRSA MODEL

The FRSA model for the charge-exchange excitations and the  $\beta$ -decay was already introduced in Refs. [24, 38] and in Ref. [25, 39], respectively. In the present study of the  $\beta$ -decay of even-even nuclei, this method is applied for the prediction of the  $\beta xn$  emission probabilities.

The  $\beta xn$  emission is a multistep process consisting of (a) the  $\beta$ -decay of the parent nucleus ( $N, Z$ ) which results in feeding the excited states of the daughter nucleus ( $N - 1, Z + 1$ ) followed by the (b)  $\beta xn$  emissions to the ground state and/or (c)  $\gamma$ -deexcitation to the ground state of the product nucleus ( $N - 1 - X, Z + 1$ ). The starting point is the HF-BCS calculation [40] of the ground state within a spherical symmetry assumption. The continuous part of the single-particle spectrum is discretized by diagonalizing the HF Hamiltonian on a harmonic oscillator basis. In the particle-hole (p-h) channel we use the Skyrme interaction with the tensor components and their inclusion leads to the modification of the spin-orbit potential [41–43]. The pairing correlations are generated by the density-dependent zero-range force

$$V_{pair}(\mathbf{r}_1, \mathbf{r}_2) = V_0 \left( 1 - \eta \left( \frac{\rho(r_1)}{\rho_0} \right)^\gamma \right) \delta(\mathbf{r}_1 - \mathbf{r}_2), \quad (1)$$

where  $\rho_0$  is the nuclear saturation density. The values of  $V_0$ ,  $\eta$  and  $\gamma$  are fixed to reproduce the odd-even mass difference of the studied nuclei [44, 45]. To calculate binding energies of the daughter nucleus  $B(N - 1, Z + 1)$  and the final nucleus  $B(N - 1 - X, Z + 1)$ , the blocking of the BCS

ground states [40, 46] is taken into account. Finally, the calculated  $Q_\beta$ -value and the neutron separation energies are given by

$$Q_\beta = \Delta M_{n-H} + B(Z + 1, N - 1) - B(Z, N), \quad (2)$$

$$S_{xn} = B(Z + 1, N - 1) - B(Z + 1, N - 1 - X). \quad (3)$$

$\Delta M_{n-H} = 0.782$  MeV is the mass difference between the neutron and the hydrogen atom.

Constructing the QRPA equations on the basis of HF-BCS quasiparticle states of the parent (even-even) nucleus ( $N, Z$ ) is the standard procedure [47]. The residual interactions in the p-h channel and the particle-particle channel are derived consistently from the Skyrme EDF. The eigenvalues of the QRPA equations are found numerically as the roots of the FRSA secular equation for the cases of electric excitations [22, 44] and charge-exchange excitations [24, 38]. It enables us to perform QRPA calculations in very large two-quasiparticle (2QP) spaces. In particular, the cut-off of the discretized continuous part of the single-particle spectra is performed at the energy of 100 MeV. This is sufficient for exhausting the Ikeda sum rule  $S_- - S_+ = 3(N - Z)$ . A rather complete list of FRSA features can be found in Ref. [25].

To take into account the phonon-phonon coupling (PPC) effects we follow the basic QPM ideas [15, 20]. The Hamiltonian can be diagonalized in a space spanned by states composed of one and two QRPA phonons [25],

$$\begin{aligned} \Psi_\nu(JM) = & \left( \sum_i R_i(J\nu) Q_{JM i}^+ \right. \\ & \left. + \sum_{\lambda_1 i_1 \lambda_2 i_2} P_{\lambda_2 i_2}^{\lambda_1 i_1}(J\nu) \left[ Q_{\lambda_1 \mu_1 i_1}^+ \bar{Q}_{\lambda_2 \mu_2 i_2}^+ \right]_{JM} \right) |0\rangle, \quad (4) \end{aligned}$$

where  $\lambda$  denotes the total angular momentum and  $\mu$  is its z-projection in the laboratory system. The ground state of the parent nucleus ( $N, Z$ ) is the QRPA phonon vacuum  $|0\rangle$ . The wave functions  $Q_{\lambda \mu i}^+ |0\rangle$  of the one-phonon excited states of the daughter nucleus ( $N - 1, Z + 1$ ) are described as linear combinations of 2QP configurations;  $\bar{Q}_{\lambda \mu i}^+ |0\rangle$  is a one-phonon electric excitation of the parent nucleus ( $N, Z$ ). The normalization condition for the wave functions (4) is

$$\sum_i R_i^2(J\nu) + \sum_{\lambda_1 i_1 \lambda_2 i_2} (P_{\lambda_2 i_2}^{\lambda_1 i_1}(J\nu))^2 = 1. \quad (5)$$

For the unknown amplitudes  $R_i(J\nu)$  and  $P_{\lambda_2 i_2}^{\lambda_1 i_1}(J\nu)$  the variational principle leads to the set of linear equations with the rank equal to the number of one- and two-phonon configurations, and for its solution it is required to compute the Hamiltonian matrix elements coupling one- and two-phonon configurations [25, 48]. The equations have the same form as the canonical QPM equations [15, 20], where the single-particle spectrum and the

residual interaction are derived from the same Skyrme EDF.

In the allowed GT approximation, the  $\beta^-$ -decay rate is expressed by summing up the probabilities (in units of  $G_A^2/4\pi$ ) of the energetically allowed transitions ( $E_k^{GT} \leq Q_\beta$ ) weighted with the integrated Fermi function

$$T_{1/2}^{-1} = \sum_k \lambda_{if}^k = D^{-1} \left( \frac{G_A}{G_V} \right)^2 \times \sum_k f_0(Z+1, A, E_k^{GT}) B(GT)_k, \quad (6)$$

$$E_k^{GT} = Q_\beta - E_{1_k^+}, \quad (7)$$

where  $\lambda_{if}^k$  is the partial  $\beta^-$ -decay rate,  $G_A/G_V=1.25$  is the ratio of the weak axial-vector and vector coupling constants and  $D=6147$  s (see Ref. [49]).  $E_{1_k^+}$  denotes the excitation energy of the daughter nucleus. As proposed in Ref. [50], this energy can be estimated by the following expression:

$$E_{1_k^+} \approx E_k - E_{2QP, \text{lowest}}, \quad (8)$$

where  $E_k$  are the  $1_k^+$  eigenvalues of the QRPA equations, or of the equations taking into account the two-phonon configurations (4), and  $E_{2QP, \text{lowest}}$  corresponds the lowest 2QP energy. The spin-parity of the lowest 2QP state is, in general, different from  $1^+$ . The wave functions allow us to determine GT transitions whose operator is  $\hat{O}_- = \sum_{i,m} t_-(i) \sigma_m(i)$ .

$$B(GT)_k = \left| \langle N-1, Z+1; 1_k^+ | \hat{O}_- | N, Z; 0_{gs}^+ \rangle \right|^2. \quad (9)$$

Because of taking into account the tensor correlation effects within the  $1p-1h$  and  $2p-2h$  configurational spaces, any quenching factors are redundant [14].

The difference in the characteristic time scales of the  $\beta$  decay and subsequent neutron emission processes justifies an assumption of their statistical independence. As proposed in Ref. [51], the  $P_{xn}$  probability of the  $\beta xn$  emission accompanying the  $\beta$  decay to the excited states in the daughter nucleus can be expressed as

$$P_{xn} = T_{1/2} D^{-1} \left( \frac{G_A}{G_V} \right)^2 \times \sum_{k'} f_0(Z+1, A, E_{k'}^{GT}) B(GT)_{k'}, \quad (10)$$

where the GT transition energy ( $E_{k'}^{GT}$ ) is located within the neutron emission window  $Q_{\beta xn} \equiv Q_\beta - S_{xn}$ . For  $P_{1n}$  we have  $Q_{\beta 2n} \leq E_{k'}^{GT} \leq Q_{\beta n}$ , while for  $P_{xn}$  this becomes  $Q_{\beta xn} \leq E_{k'}^{GT} \leq Q_{\beta x-1n}$ . Since we neglect the  $\gamma$ -deexcitation of the daughter nucleus, some overestimation of the resulting  $P_{xn}$  values can be obtained [11]. The study of the  $\gamma$ -deexcitation influence on the  $P_{xn}$  values within our approach is in progress.

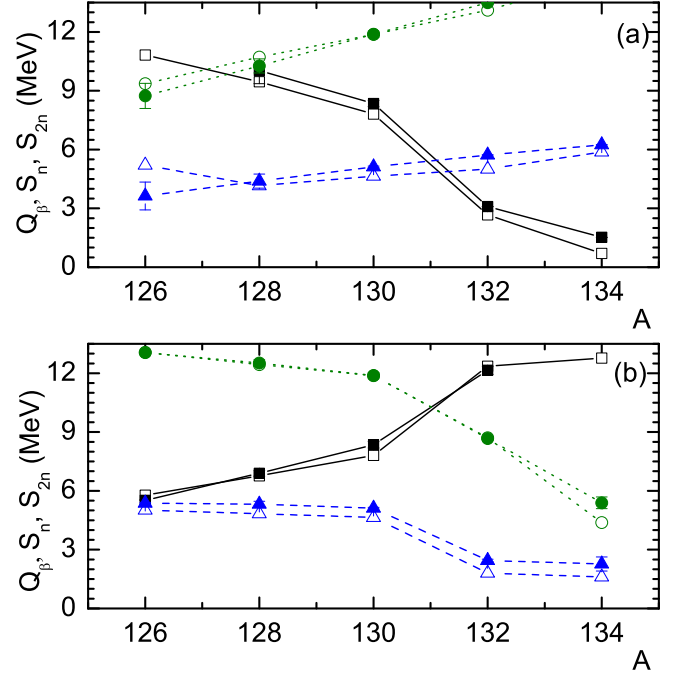


FIG. 1: (color online) Calculated  $\beta$ -decay windows  $Q_\beta$  of the parent nuclei (squares), one- (triangles) and two- (circles) neutron separation energies for the daughter nuclei. The upper and lower panels correspond to the even  $N = 82$  isotones and the even Cd isotopes, respectively. Results of the HF-BCS calculations are denoted by the open symbols. Experimental data (filled symbols) are taken from Ref. [54].

### III. DETAILS OF CALCULATIONS

As the parameter set in the particle-hole channel, we use the Skyrme EDF T43 which takes into account the tensor term [43]. The T43 set is one of 36 parametrizations, covering a wide range of the parameter space of the isoscalar and isovector tensor term added with refitting the parameters of the central interaction, where a fit protocol is very similar to that of the successful SLy parametrizations. The spin-isospin Landau parameter is given by

$$G'_0 = -N_0 \left[ \frac{1}{4} t_0 + \frac{1}{24} t_3 \rho^{\alpha_3} + \frac{1}{8} k_F^2 (t_1 - t_2) \right], \quad (11)$$

where  $N_0 = 2k_F m^* / \pi^2 \hbar^2$  is the level density, with  $k_F$  being the Fermi momentum and  $m^*$  the nucleon effective mass. At saturation density ( $\rho = \rho_0$ ), the set T43 predicts enough positive value for  $G'_0 = 0.14$  and it gives a reasonable description of properties of the GT and charge-exchange spin-dipole resonances [52]. Using the PPC effects within the FRSA model, the T43 set gives a reasonable agreement with experimental data for the  $\beta$ -decay half-life of the neutron-rich doubly-magic nucleus  $^{132}\text{Sn}$ , see Sec. IV A. It is worth mentioning that the first study of the strong impact of the tensor correlations on the  $^{132}\text{Sn}$  half-life has been done in [53].

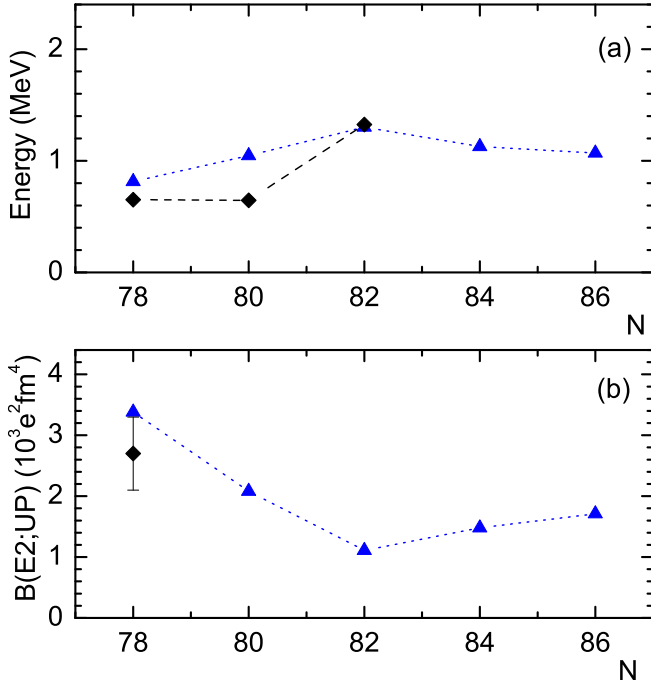


FIG. 2: (color online) Energies and  $B(E2)$  values for up-transitions to the  $[2_1^+]_{QRPA}$  states in the neutron-rich Cd isotopes. Results of the QRPA calculations are denoted by the triangles. Experimental data (diamonds) are taken from Refs. [55–57].

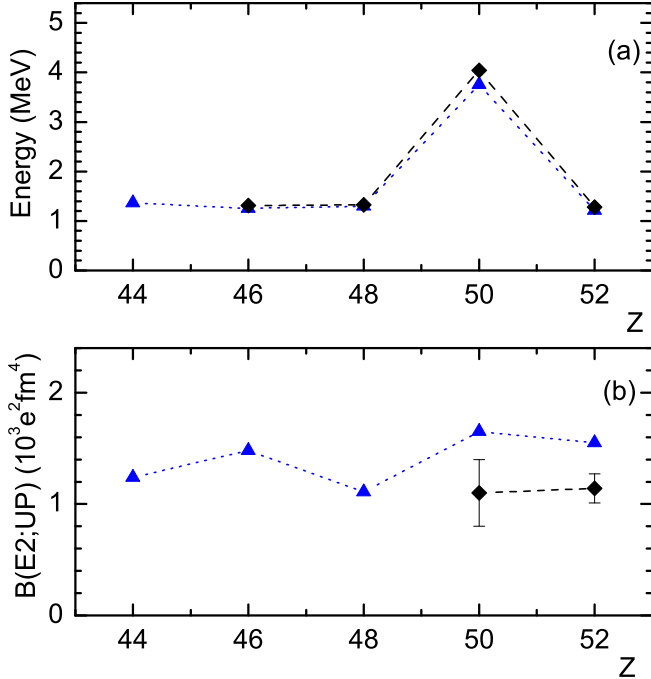


FIG. 3: Same as Fig. 2, but for the neutron-rich  $N = 82$  isotones. Experimental data (diamonds) are taken from Refs. [55, 58–60].

The pairing correlations are generated by a surface-

peaked pairing force (1) with  $\eta = 1$ ,  $\gamma = 1$  and the value  $\rho_0 = 0.16 \text{ fm}^{-3}$  for the nuclear saturation density. Using the soft cutoff at 10 MeV above the Fermi energies, the pairing strength is fixed to be  $V_0 = -870 \text{ MeV fm}^3$  in order to fit the experimental neutron pairing gaps of  $^{126,128}\text{Cd}$ ,  $^{130}\text{Sn}$ ,  $^{132}\text{Te}$  obtained by the three-point formula [24, 38].

The correct description of the  $Q_\beta$  values for the parent nuclei and the neutron separation energies ( $S_{xn}$ ) for the daughter nuclei is the important ingredient for the reliable prediction of the  $P_{2n}/P_{1n}$  ratios. The binding energies of the daughter and final nuclei are calculated with the blocking effect for unpaired nucleons [40, 46]. For  $^{126}\text{Rh}$ ,  $^{128}\text{Ag}$ ,  $^{126,128,130}\text{In}$ ,  $^{132}\text{Sb}$  and  $^{134}\text{I}$ , the neutron quasiparticle blocking is based on filling the  $1h_{11/2}$  subshell and the  $2f_{7/2}$  subshell should be blocked for  $^{132,134}\text{In}$ . The proton  $1g_{9/2}$  and  $1g_{7/2}$  subshells are chosen to be blocked in the cases of the Rh, Ag, In isotopes and the Sb, I isotopes, respectively. The calculated  $Q_\beta$ ,  $S_n$  and  $S_{2n}$  values of the  $\beta$ -decays of the even Cd isotopes and the  $N = 82$  isotones are compared with the experimental data [54] in Fig. 1. The existing experimental data show a different  $A$ -behavior, namely, the 6.6-time reduction of  $Q_\beta$  values from  $^{128}\text{Pd}$  to  $^{134}\text{Te}$  and the gradual reduction of  $Q_\beta$  values with decreasing neutron number for the Cd isotopes. The results of the HF-BCS calculation with the T43 EDF are in a reasonable agreement with the experimental data.

In order to construct the wave functions (4) of the low-energy  $1^+$  states, in the present study we assume only the  $[1_i^+ \otimes 2_i^+]_{QRPA}$  terms for separating the sole impact of the quadrupole-phonon coupling. All one- and two-phonon configurations with the excitation energy of the daughter nucleus  $E_{1_k^+}$  up to 16 MeV are included. We have checked that the inclusion of the high-energy configurations leads to minor effects on the half-life values. As it is pointed out in Ref. [25], the  $[1_1^+ \otimes 2_1^+]_{QRPA}$  configuration is the important ingredient for the half-life description since the  $[2_1^+]_{QRPA}$  state is the lowest collective excitation which leads to the minimal two-phonon energy and the maximal Hamiltonian matrix elements for coupling of the one- and two-phonon configurations.

It is interesting to examine the energies and transition probabilities of the  $[2_1^+]_{QRPA}$  states of the neutron-rich Cd isotopes (see Fig. 2). There is a significant increase of the  $2_1^+$  energy of  $^{130}\text{Cd}$ . It corresponds to a standard evolution of the  $2_1^+$  energy near closed shells. In all five nuclei, the  $2_1^+$  wave functions are dominated by the proton configuration  $\{1g_{9/2}, 1g_{9/2}\}_\pi$  (>73%). The closure of the neutron subshell  $1h_{11/2}$  in  $^{130}\text{Cd}$ , leads to the vanishing of the neutron pairing and as a result the lowest neutron 2QP energy  $\{2f_{7/2}, 1h_{11/2}\}_\nu$  is larger than the lowest neutron 2QP energies  $\{1h_{11/2}, 1h_{11/2}\}_\nu$  in  $^{128}\text{Cd}$  and  $\{2f_{7/2}, 2f_{7/2}\}_\nu$  in  $^{132}\text{Cd}$ . Correspondingly the  $2_1^+$  state of  $^{130}\text{Cd}$  has noncollective structure with the  $\{1g_{9/2}, 1g_{9/2}\}_\pi$  domination (about 96%) and the  $B(E2)$  value is reduced. As the data for the Cd isotopes are very scarce, the  $N = 82$  isotones are used for reference.

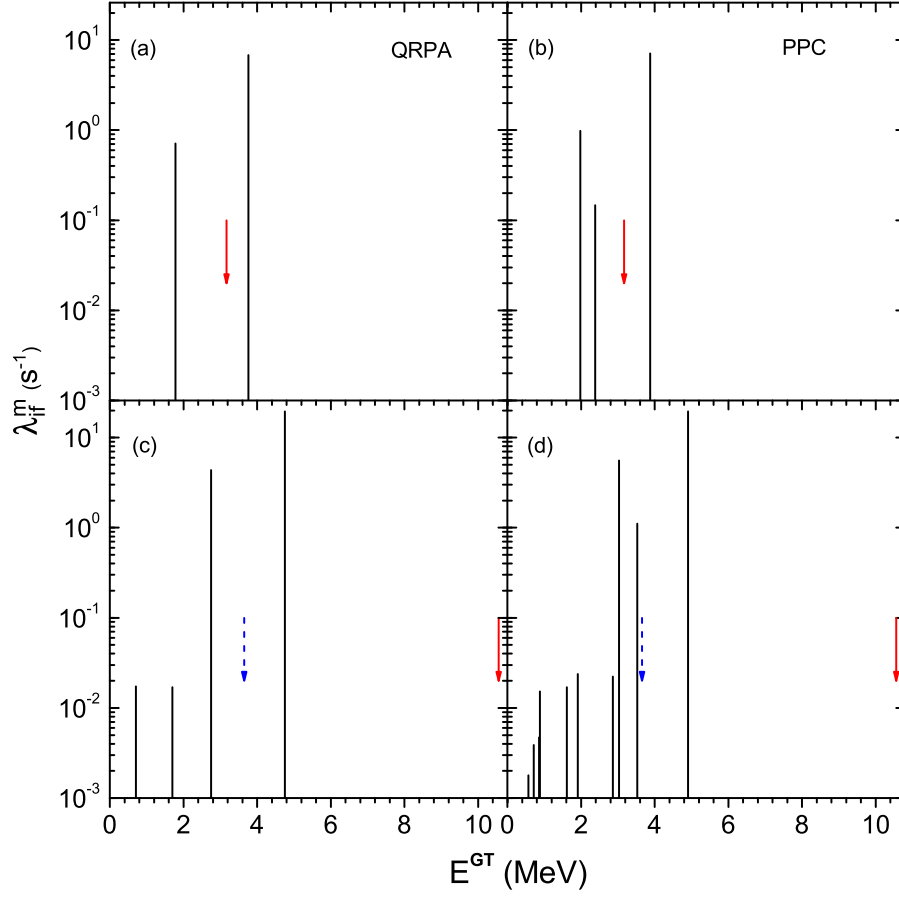


FIG. 4: (color online) The phonon-phonon coupling effect on the  $\beta$ -transition rates in  $^{130}\text{Cd}$  (the upper panels) and  $^{132}\text{Cd}$  (the lower panels). The left and right panels correspond to the calculations within the QRPA and taking into account the  $[1_i^+ \otimes 2_{i'}^+]_{QRPA}$  configurations, respectively. The calculated  $Q_{\beta 1n}$  and  $Q_{\beta 2n}$  energies are denoted by the solid and dashed arrows, respectively.

Results of QRPA calculation with T43 EDF and the experimental data [55, 58–60] are shown in Fig. 3. The calculated values are in a reasonable agreement with the data. Moving along the neutron-rich  $N = 82$  isotones chain one can find that  $2_1^+$  states in  $^{126}\text{Ru}$ ,  $^{128}\text{Pd}$  and  $^{130}\text{Cd}$  as is discussed above, have a noncollective structure with a domination of the  $\{1g_{9/2}, 1g_{9/2}\}_\pi$  configuration. In  $^{132}\text{Sn}$ , the main configurations are the neutron  $\{2f_{7/2}, 1h_{11/2}\}_\nu$  (56%) and the proton  $\{2d_{5/2}, 1g_{9/2}\}_\pi$  (37%) ones. In  $^{134}\text{Te}$ , the  $2_1^+$  state is dominated by the lowest 2QP component  $\{1g_{7/2}, 1g_{7/2}\}_\pi$ . The structure peculiarities are reflected in the  $B(E2)$  behavior in this chain. We find a satisfactory description of the isotonic dependence of the  $2_1^+$  energy near the closed proton shell.

#### IV. RESULTS

Using the same set of parameters the main features of the  $\beta$ -decay and available  $\beta xn$  rates are described for the neutron-rich nuclei  $^{132}\text{Sn}$ ,  $^{126,128,130,132,134}\text{Cd}$ ,  $^{128}\text{Pd}$  and  $^{126}\text{Ru}$ . The integral  $\beta$ -decay observables are sub-

stantially defined by the structure of the  $\beta$ -strength function. Fig.4 depicts the  $\beta$ -strength function of  $^{130,132}\text{Cd}$  (in terms of the transition rate) calculated a), c) within the QRPA and b), d) with the  $[1_i^+ \otimes 2_{i'}^+]_{QRPA}$  configurations taken into account.

For  $^{130}\text{Cd}$ , the QRPA strength function has a rather simple two-peak structure, the main transition to the  $[1_1^+]_{QRPA}$  state is built on the  $\{\pi 1g_{9/2}, \nu 1g_{7/2}\}$  configuration. Inclusion of the PPC shifts main peak by +120 keV increasing its amplitude by 5% and also an additional low rate peak at  $E_2^{GT} = 2.4$  MeV comes from the  $[1_1^+ \otimes 2_1^+]_{QRPA}$  configuration (93%). Thus an additional peak is dominated by the four-quasiparticle configuration  $\{\pi 1g_{9/2}, \pi 1g_{9/2}, \pi 1g_{9/2}, \nu 1g_{7/2}\}$ . On the other hand, the main contribution to the GT matrix element comes from the one-phonon configuration  $[1_1^+]_{QRPA}$  which exhausts about 6% of the  $1_2^+$  wave function. These changes are translated into the corresponding half-life reduction and  $P_{tot}$  growth. This will be discussed in the next subsections. As can be seen from Fig.4, we get the similar tendency of the QRPA strength function in the case of  $^{132}\text{Cd}$ . However there are remarkable changes in the val-

TABLE I: The phonon-phonon coupling effect on  $\beta$ -decay half-lives of the neutron-rich Cd isotopes. Experimental data are taken from [28].

Nucleus	Half-life (ms)		
	QRPA	PPC	Expt.
$^{126}\text{Cd}$	334	263	$513 \pm 6$
$^{128}\text{Cd}$	212	180	$245 \pm 5$
$^{130}\text{Cd}$	133	121	$127 \pm 2$
$^{132}\text{Cd}$	42	38	$82 \pm 4$
$^{134}\text{Cd}$	36	32	$65 \pm 15$

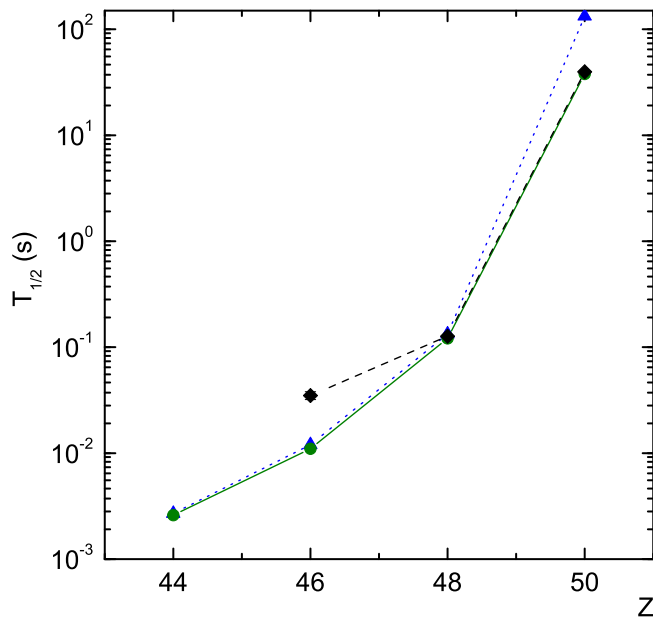


FIG. 5: (color online) The phonon-phonon coupling effect on  $\beta$ -decay half-lives of the neutron-rich  $N = 82$  isotones. The circles correspond to the half-lives calculated with inclusion of the  $[1_1^+ \otimes 2_{\nu}^+]_{QRPA}$  configurations, the triangles are the QRPA calculations. Experimental data (diamonds) are from Refs. [28, 61].

ues of the  $Q_{\beta 1n}$  and  $Q_{\beta 2n}$  windows. It is seen that the calculated neutron-emission probability ( $P_{tot}$ ) exhausts 100% since all the GT transition energies are less than  $Q_{\beta 1n}$ . The additional (two-phonon) peak leads to the  $P_{2n}/P_{1n}$  increase, see Sec. IV B.

### A. $\beta$ -decay half-lives

For  $^{126,128,130,132,134}\text{Cd}$ , the results of our calculations and experimental data [28] are shown in Table 1. First, the half-lives are studied within the one-phonon approximation. At a qualitative level, our results reproduce

the experimental mass dependence of the half-lives. The largest contribution ( $>80\%$ ) in all the calculated half-lives comes from the  $[1_1^+]_{QRPA}$  state. The dominant configuration of the  $[1_1^+]_{QRPA}$  states is  $\{\pi 1g_{9/2}, \nu 1g_{7/2}\}$  with the contribution of about 99 %, and  $\log ft \approx 2.9$  in all the Cd isotopes considered. Let us consider how to explain the 3.2-time reduction of calculated half-life values from  $^{130}\text{Cd}$  to  $^{132}\text{Cd}$ , see Table 1. The  $\{\pi 1g_{9/2}, \nu 1g_{7/2}\}$  energy is equal to 7.5 MeV for  $^{130}\text{Cd}$  and 9.5 MeV for  $^{132}\text{Cd}$ . Also we find that the lowest 2QP energy is either the  $\{\pi 1g_{9/2}, \nu 1h_{11/2}\}$  value of 3.4 MeV for  $^{130}\text{Cd}$ , or  $\{\pi 1g_{9/2}, \nu 2f_{7/2}\}$  value of 1.9 MeV for  $^{132}\text{Cd}$ . As a result, the excitation energy of the first  $1^+$  state is increased from  $^{130}\text{In}$  to  $^{132}\text{In}$ . Therefore, the 4.6 MeV increase of the  $Q_{\beta}$  values (see Fig. 1) plays the key role to explain this half-life reduction. The analysis within the one-phonon approximation can help to explain the main peculiarities of the half-lives A-dependence, but it is only a rough estimate.

Let us now discuss the extension of the space to one- and two-phonon configurations on the half-lives. As expected, the largest contribution ( $>70\%$ ) in half-life comes from the  $1_1^+$  state calculated with the PPC. The dominant contribution in the wave function of the first  $1^+$  state comes from the  $[1_1^+]_{QRPA}$  configuration, but the  $[1_1^+ \otimes 2_1^+]_{QRPA}$  contribution is appreciable. Inclusion of the two-phonon terms results in a decrease of the  $1_1^+$  energy. The well-known experimental characteristics of the  $1_1^+$  state in  $^{130}\text{In}$  is a stringent test for the existing microscopic approaches [62]. Results of FRSA model with the T43 EDF ( $E_{1_1^+} = 3.9$  MeV and  $\log ft = 3.0$ ) can be compared with the experimental excitation energy  $E_{1_1^+} = 2.12$  MeV and  $\log ft = 4.1$  [27]. The calculated two-quasiparticle energy and unperturbed B(GT) value are too large to be properly renormalized the inclusion of the two-phonon configurations. One may possibly seek for improvements of the  $T = 0$  pairing term in the EDF used. Table 1 shows the half-life reduction as an effect of the quadrupole-phonon coupling, see, e.g., Fig. 4. The calculated half-life of  $^{130}\text{Cd}$  is in excellent agreement with the experimental data [28]. The discrepancies between measured and calculated half-lives of  $^{126,132,134}\text{Cd}$  are due to total neglect of the first-forbidden transitions.

It is worth to mention that the EDF T43 within the QRPA gives a satisfactory agreement with experimental data for the  $\beta$ -decay half-life of the neutron-rich doubly-magic nucleus  $^{132}\text{Sn}$  [53]. The PPC effect results in a improvement of the half-life description, see Fig. 5. As can be seen from Table 1 and Fig. 5, there are different behavior of the existing experimental half-lives [28, 61], namely, the 313-time reduction of half-life values from  $^{132}_{50}\text{Sn}$  to  $^{130}_{48}\text{Cd}$  and the gradual reduction of half-lives with increasing neutron number for  $^{126,128,130}\text{Cd}$ . One can see that FRSA model with the T43 EDF reproduces this behaviour and our results predict the half-lives for  $^{128}_{46}\text{Pd}$  and  $^{126}_{44}\text{Ru}$ . Further an improvement can be achieved if the first-forbidden transitions are taken into account [10].



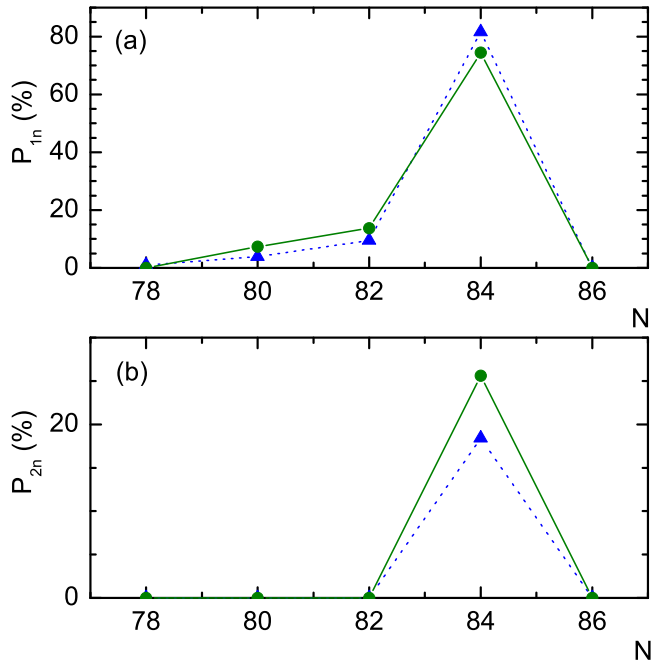


FIG. 6: (color online) The phonon-phonon coupling effect on  $\beta$ -delayed neutron-emission probabilities of the neutron-rich Cd isotopes. The circles correspond to the probabilities calculated with inclusion of the  $[1_i^+ \otimes 2_j^+]_{QRPA}$  configurations, the triangles are the QRPA calculations.

It is planned to extend our formalism including the first-forbidden transitions.

### B. Probabilities of the $\beta$ -delayed neutron emission

An additional constraints on the  $\beta$ -strength function are given by the total and multi-neutron emission probabilities. The well-known experimental probabilities are  $P_{tot} = 3.5 \pm 1.0\%$  for  $^{130}\text{Cd}$  [27] and  $60 \pm 15\%$  for  $^{132}\text{Cd}$  [26]. The calculated  $P_{1n,2n}$  values are displayed in Fig. 6. For  $^{126}\text{Cd}$ , one has to mention a non-zero  $P_{tot}$  value less than 1%. For  $^{130}\text{Cd}$ , the calculated  $P_{tot}$  value of 13.7% is higher than the experimental value of 3.5% [27] which may indicate the necessity of including the  $T = 0$  pairing interaction. For all considered isotopes we obtain the maximal  $P_{1n}$  and  $P_{2n}$  values in the case of  $^{132}\text{Cd}$ . The redistribution of the QRPA estimate in favor of  $P_{2n}$  occurs when the PPC effect is included:  $P_{2n} = 25.6\%$  compared to  $P_{1n} = 74.4\%$ . This differs from the DF3a+cQRPA prediction by Ref. [63] which gives  $P_{1n} = 84.13\%$ ,  $P_{2n} = 0.14\%$ . Also, it is interesting to compare the  $P_{2n}/P_{1n}$  ratios. They are 0.002 in Ref. [63] and 0.34 in the present calculation. The difference between the predictions of two models can be explained by the sensitivity of multi-neutron delayed emission to the details of the  $\beta$ -strength function and the neutron separation energies. Also further from the closed shell ( $^{134}\text{Cd}$ ) one can not neglect the increasing contribution

of the first-forbidden transition known to reduce the  $P_{tot}$  value [11, 33, 63] and substantially redistributing  $P_{xn}$  values. As is shown in Ref. [63], the DF3a+cQRPA calculation gives  $P_{1n} = 32.75\%$ ,  $P_{2n} = 47.47\%$  and  $P_{3n} = 7.12\%$ .

It would be instructive to study the PPC effect on the  $P_{1n,2n}$  values of the neutron-rich nuclei. For  $^{126,128,130}\text{Cd}$  within the QRPA there are two main GT decays which define the  $P_{tot}$  values (see for example, Fig. 4). The inclusion of the PPC has a stronger influence on the energy shift of the  $1_3^+$  state which is mainly built on the  $[1_2^+]_{QRPA}$  configuration. Also the two-phonon state  $1_2^+$  appears. Both effects increase the  $P_{tot}$  value. In the case of  $^{132}\text{Cd}$  these dynamic features of  $1_2^+$  and  $1_3^+$  states are responsible for increasing the  $P_{2n}$  value. The QRPA value  $P_{2n}/P_{1n} = 0.22$  is replaced by 0.34 with the PPC included. Notice that  $P_{2n}/P_{1n} = 0.29$  if the  $1_2^+$  state is not taken into account.

## V. CONCLUSIONS

Starting from the Skyrme mean-field calculations, we have studied the effects of the phonon-phonon coupling on the properties of the  $\beta$ -delayed multi-neutron emission and, in particular, on  $P_{2n}/P_{1n}$  ratios of nuclei in the mass range  $A \approx 130$ . The finite-rank separable approach to the QRPA problem enables one to perform the calculations in very large configurational spaces.

The parametrization T43 of the Skyrme interaction is used for all calculations in connection with the surface-peaked zero-range pairing interaction. In particular, we study the multi-neutron emission in the  $^{132}\text{Cd}$  in comparison with  $N = 82$  isotone  $^{130}\text{Cd}$ . We have found a significant two-neutron emission for  $^{132}\text{Cd}$ , the effect which was predicted within the FRDM+QRPA and the DF3+cQRPA before. Notice, that as well as in the DF3+cQRPA calculations, our results from the Skyrme interaction are in reasonable agreement with experimental half-lives. It is the first successful description obtained with the Skyrme interaction for the experimental neutron-emission probabilities. The coupling between one- and two-phonon terms in the wave functions of  $1^+$  states is shown to be essential. The QRPA underestimates the  $P_{2n}/P_{1n}$  values. Inclusion of the two-phonon configurations produces an impact on the  $P_{2n}$  value which leads to the 55% increase of the  $P_{2n}/P_{1n}$  ratio. For  $^{126,128,130,132,134}\text{Cd}$ , the maximal  $P_{1n}$  and  $P_{2n}$  values are obtained in the case of  $^{132}\text{Cd}$ . For  $^{126}\text{Cd}$ , a nonzero probability of the neutron emission is found.

We conclude that the present approach makes it possible to perform the new microscopic analysis of the rates of the  $\beta$ -delayed multi-neutron emission. The model can be extended by enlarging the variational space for the  $1^+$  states with the inclusion of the two-phonon configurations constructed from phonons with monopole, dipole and octupole multipolarities. The computational developments that would allow us to conclude on this point are underway.

## Acknowledgments

We thank Nguyen Van Giai, Yu.E. Penionzhkevich, H. Sagawa and D. Verney for useful discussions. This work

is supported by the Russian Science Foundation (Grant No. RSF-16-12-10161).

- 
- [1] K. Langanke, and G. Martínez-Pinedo, *Rev. Mod. Phys.* **75**, 819 (2003).
  - [2] V. I. Goldansky, *Nucl. Phys.* **19**, 482 (1960).
  - [3] R. E. Azuma, L. C. Carraz, P. G. Hansen, B. Jonson, K.-L. Kratz, S. Mattsson, G. Nyman, H. Ohm, H. L. Ravn, A. Schröder, and W. Ziegert, *Phys. Rev. Lett.* **43**, 1652 (1979).
  - [4] C. Detraz, M. Epherre, D. Guillemaud, P. G. Hansen, B. Jonson, R. Klapisch, M. Langevin, S. Mattsson, F. Naulin, G. Nyman, A. M. Poskanzer, H. L. Ravn, M. de Saint-Simon, K. Takahashi, C. Thibault, and F. Touchard, *Phys. Lett. B* **94**, 307 (1980).
  - [5] Yu. S. Lyutostansky, V. K. Sirotkin, and I. V. Panov, *Phys. Lett. B* **161**, 9 (1985).
  - [6] A. Spyrou, Z. Kohley, T. Baumann, D. Bazin, B. A. Brown, G. Christian, P. A. DeYoung, J. E. Finck, N. Frank, E. Lunderberg, S. Mosby, W. A. Peters, A. Schiller, J. K. Smith, J. Snyder, M. J. Strongman, M. Thoennessen, and A. Volya, *Phys. Rev. Lett.* **108**, 102501 (2012).
  - [7] F. M. Marqués, N. A. Orr, N. L. Achouri, F. Delaunay, and J. Gibelin, *Phys. Rev. Lett.* **109**, 239201 (2012).
  - [8] C. A. Bertulani, and V. Zelevinsky, *Nature* **532**, 448 (2016).
  - [9] R. Caballero-Folch, C. Domingo-Pardo, J. Agramunt, A. Algora, F. Ameil, A. Arcones, Y. Ayyad, J. Benlliure, I. N. Borzov, M. Bowry, F. Calviño, D. Cano-Ott, G. Cortés, T. Davinson, I. Dillmann, A. Estrade, A. Evdokimov, T. Faestermann, F. Farinon, D. Galaviz, A. R. García, H. Geissel, W. Gelletly, R. Gernhäuser, M. B. Gómez-Hornillos, C. Guerrero, M. Heil, C. Hinke, R. Knöbel, I. Kojouharov, J. Kurcewicz, N. Kurz, Yu. A. Litvinov, L. Maier, J. Marganec, T. Marketin, M. Marta, T. Martínez, G. Martínez-Pinedo, F. Montes, I. Mukha, D. R. Napoli, C. Nociforo, C. Paradela, S. Pietri, Zs. Podolyák, A. Prochazka, S. Rice, A. Riego, B. Rubio, H. Schaffner, Ch. Scheidenberger, K. Smith, E. Sokol, K. Steiger, B. Sun, J. L. Taín, M. Takechi, D. Testov, H. Weick, E. Wilson, J. S. Winfield, R. Wood, P. Woods, and A. Yeremin, *Phys. Rev. Lett.* **117**, 012501 (2016).
  - [10] I. N. Borzov, *Phys. Rev. C* **67**, 025802 (2003).
  - [11] I.N. Borzov, *Phys. Rev. C* **71**, 065801 (2005).
  - [12] T. Wakasa, H. Sakai, H. Okamura, H. Otsu, S. Fujita, S. Ishida, N. Sakamoto, T. Uesaka, Y. Satou, M. B. Greenfield, and K. Hatanaka, *Phys. Rev. C* **55**, 2909 (1997).
  - [13] M. Ichimura, H. Sakai, and T. Wakasa, *Prog. Part. Nucl. Phys.* **56**, 446 (2006).
  - [14] G. F. Bertsch and I. Hamamoto, *Phys. Rev. C* **26**, 1323 (1982).
  - [15] V. A. Kuzmin and V. G. Soloviev, *J. Phys.* **G10**, 1507 (1984).
  - [16] S. Drozd, F. Osterfeld, J. Speth, and J. Wambach, *Phys. Lett.* **B189**, 271 (1987).
  - [17] G. Coló, Nguyen Van Giai, P. F. Bortignon, and R. A. Broglia, *Phys. Rev. C* **50**, 1496 (1994).
  - [18] G. Coló, H. Sagawa, Nguyen Van Giai, P. F. Bortignon, and T. Suzuki, *Phys. Rev. C* **57**, 3049 (1998).
  - [19] Y. F. Niu, G. Coló, M. Brenna, P. F. Bortignon, and J. Meng, *Phys. Rev. C* **85**, 034314 (2012).
  - [20] V. G. Soloviev, *Theory of Atomic Nuclei: Quasiparticles and Phonons* (Institute of Physics, Bristol and Philadelphia, 1992).
  - [21] V. A. Kuzmin and V. G. Soloviev, *J. Phys.* **G11**, 603 (1985).
  - [22] Nguyen Van Giai, Ch. Stoyanov, and V. V. Voronov, *Phys. Rev. C* **57**, 1204 (1998).
  - [23] A. P. Severyukhin, V. V. Voronov, and Nguyen Van Giai, *Eur. Phys. J. A* **22**, 397 (2004).
  - [24] A. P. Severyukhin, V. V. Voronov, and Nguyen Van Giai, *Prog. Theor. Phys.* **128**, 489 (2012).
  - [25] A. P. Severyukhin, V. V. Voronov, I. N. Borzov, N. N. Arsenyev, and Nguyen Van Giai, *Phys. Rev. C* **90**, 044320 (2014).
  - [26] M. Hannawald, V. N. Fedoseyev, U. Köster, K.-L. Kratz, V. I. Mishin, W. F. Mueller, H. L. Ravn, J. Van Roosbroeck, H. Schatz, V. Sebastian, W. B. Walters, and the ISOLDE Collaboration, *Nucl. Phys. A* **688**, 578c (2001).
  - [27] I. Dillmann, K.-L. Kratz, A. Wöhr, O. Arndt, B. A. Brown, P. Hoff, M. Hjorth-Jensen, U. Köster, A. N. Ostrowski, B. Pfeiffer, D. Seweryniak, J. Shergur, W. B. Walters, and the ISOLDE Collaboration, *Phys. Rev. Lett.* **91**, 162503 (2003).
  - [28] G. Lorusso, S. Nishimura, Z. Y. Xu, A. Jungclaus, Y. Shimizu, G. S. Simpson, P.-A. Söderström, H. Watanabe, F. Browne, P. Doornenbal, G. Gey, H. S. Jung, B. Meyer, T. Sumikama, J. Taprogge, Zs. Vajta, J. Wu, H. Baba, G. Benzoni, K. Y. Chae, F. C. L. Crespi, N. Fukuda, R. Gernhäuser, N. Inabe, T. Isobe, T. Kajino, D. Kameda, G. D. Kim, Y.-K. Kim, I. Kojouharov, F. G. Kondev, T. Kubo, N. Kurz, Y. K. Kwon, G. J. Lane, Z. Li, A. Montaner-Pizá, K. Moschner, F. Naqvi, M. Nikura, H. Nishibata, A. Odahara, R. Orlandi, Z. Patel, Zs. Podolyák, H. Sakurai, H. Schaffner, P. Schury, S. Shibagaki, K. Steiger, H. Suzuki, H. Takeda, A. Wendt, A. Yagi, and K. Yoshinaga, *Phys. Rev. Lett.* **114**, 192501 (2015).
  - [29] R. Dunlop, V. Bildstein, I. Dillmann, A. Jungclaus, C. E. Svensson, C. Andreoiu, G. C. Ball, N. Bernier, H. Bidaman, P. Boubel, C. Burbadge, R. Caballero-Folch, M. R. Dunlop, L. J. Evitts, F. Garcia, A. B. Garnsworthy, P. E. Garrett, G. Hackman, S. Hallam, J. Henderson, S. Ilyushkin, D. Kisliuk, R. Krücken, J. Lassen, R. Li, E. MacConnachie, A. D. MacLean, E. McGee, M. Moukaddam, B. Olaizola, E. Padilla-Rodal, J. Park, O. Paetkau, C. M. Petrache, J. L. Pore, A. J. Radich, P. Ruotsalainen, J. Smallcombe, J. K. Smith, S. L. Tabor, A. Teigelhöfer, J. Turko, and T. Zidar, *Phys. Rev. C* **93**, 062801(R) (2016).
  - [30] A. Jungclaus, H. Grawe, S. Nishimura, P. Doornenbal, G. Lorusso, G. S. Simpson, P.-A. Söderström, T. Sumikama,



- J. Taprogge, Z. Y. Xu, H. Baba, F. Browne, N. Fukuda, R. Gernhäuser, G. Gey, N. Inabe, T. Isobe, H. S. Jung, D. Kameda, G. D. Kim, Y.-K. Kim, I. Kojouharov, T. Kubo, N. Kurz, Y. K. Kwon, Z. Li, H. Sakurai, H. Schaffner, Y. Shimizu, K. Steiger, H. Suzuki, H. Takeda, Zs. Vajta, H. Watanabe, J. Wu, A. Yagi, K. Yoshinaga, G. Benzoni, S. Bönig, K. Y. Chae, L. Coraggio, J.-M. Daugas, F. Drouet, A. Gadea, A. Gargano, S. Ilieva, N. Itaco, F. G. Kondev, T. Kröll, G. J. Lane, A. Montaner-Pizá, K. Moschner, D. Mücher, F. Naqvi, M. Niikura, H. Nishibata, A. Odahara, R. Orlandi, Z. Patel, Zs. Podolyák, and A. Wendt, *Phys. Rev. C* **94**, 024303 (2016).
- [31] P. Möller, J. R. Nix, and K.-L. Kratz, *At. Data Nucl. Data Tables* **66**, 131 (1997).
- [32] I.N. Borzov, *Nucl. Phys. A* **777**, 645 (2006).
- [33] I. N. Borzov, J. J. Cuenca-García, K. Langanke, G. Martínez-Pinedo, and F. Montes, *Nucl. Phys. A* **814**, 159 (2008).
- [34] T. Marketin, L. Huther, and G. Martínez-Pinedo, *Phys. Rev. C* **93**, 025805 (2016).
- [35] M. T. Mustonen, and J. Engel, *Phys. Rev. C* **93**, 014304 (2016).
- [36] P. Möller, B. Pfeiffer, and K.-L. Kratz, *Phys. Rev. C* **67**, 055802 (2003).
- [37] Q. Zhi, E. Caurier, J. J. Cuenca-García, K. Langanke, G. Martínez-Pinedo, and K. Sieja, *Phys. Rev. C* **87**, 025803 (2013).
- [38] A. P. Severyukhin and H. Sagawa, *Prog. Theor. Exp. Phys.* **2013**, 103D03 (2013).
- [39] A. Etile, D. Verney, N. N. Arsenyev, J. Bettane, I. N. Borzov, M. Cheikh Mhamed, P. V. Cuong, C. Delafosse, F. Didierjean, C. Gaulard, Nguyen Van Giai, A. Goasduff, F. Ibrahim, K. Kolos, C. Lau, M. Niikura, S. Roccia, A. P. Severyukhin, D. Testov, S. Tusseau-Nenez, and V. V. Voronov, *Phys. Rev. C* **91**, 064317 (2015).
- [40] P. Ring and P. Schuck, *The Nuclear Many Body Problem* (Springer, Berlin, 1980).
- [41] F. Stancu, D. M. Brink, and H. Flocard, *Phys. Lett.* **B68**, 108 (1977).
- [42] G. Colò, H. Sagawa, S. Fracasso, and P.F. Bortignon, *Phys. Lett.* **B646**, 227 (2007); *Phys. Lett.* **B668**, 457(E) (2008).
- [43] T. Lesinski, M. Bender, K. Bennaceur, T. Duguet, and J. Meyer, *Phys. Rev. C* **76**, 014312 (2007).
- [44] A. P. Severyukhin, V. V. Voronov, and Nguyen Van Giai, *Phys. Rev. C* **77**, 024322 (2008).
- [45] S. J. Krieger, P. Bonche, H. Flocard, P. Quentin, and M. S. Weiss, *Nucl. Phys.* **A517**, 275 (1990).
- [46] V. G. Soloviev, *Kgl. Dan. Vid. Selsk. Mat. Fys. Skr.* **1**, 238 (1961).
- [47] J. Terasaki, J. Engel, M. Bender, J. Dobaczewski, W. Nazarewicz, and M. Stoitsov, *Phys. Rev. C* **71**, 034310 (2005).
- [48] A. P. Severyukhin, V. V. Voronov, I. N. Borzov and Nguyen Van Giai, *Rom. Journ. Phys.* **58**, 1048 (2013).
- [49] J. Suhonen, *From Nucleons to Nucleus* (Springer-Verlag, Berlin, 2007).
- [50] J. Engel, M. Bender, J. Dobaczewski, W. Nazarewicz, and R. Surman, *Phys. Rev. C* **60**, 014302 (1999).
- [51] A. C. Pappas and T. Sverdrup, *Nucl. Phys.* **A188**, 48 (1972).
- [52] C.L. Bai, H.Q. Zhang, H. Sagawa, X.Z. Zhang, G. Colò and F.R. Xu, *Phys. Rev.* **C83**, 054316 (2011).
- [53] F. Minato and C. L. Bai, *Phys. Rev. Lett.* **110**, 122501 (2013); *Phys. Rev. Lett.* **116**, 089902(E) (2016).
- [54] M. Wang, G. Audi, A. H. Wapstra, F. G. Kondev, M. MacCormick, X. Xu, and B. Pfeiffer, *Chin. Phys. C* **36**, 1603 (2012).
- [55] A. Jungclaus, L. Cáceres, M. Górska, M. Pfützner, S. Pietri, E. Werner-Malento, H. Grawe, K. Langanke, G. Martínez-Pinedo, F. Nowacki, A. Poves, J. J. Cuenca-García, D. Rudolph, Z. Podolyak, P. H. Regan, P. Deltsov, S. Lalkovski, V. Modamio, J. Walker, P. Bednarczyk, P. Doornenbal, H. Geissel, J. Gerl, J. Grebosz, I. Kojouharov, N. Kurz, W. Prokopowicz, H. Schaffner, H. J. Wollersheim, K. Andgren, J. Benlliure, G. Benzoni, A. M. Bruce, E. Casarejos, B. Cederwall, F. C. L. Crespi, B. Hadinia, M. Hellström, R. Hoischen, G. Ilie, J. Jolie, A. Khaplanov, M. Kmiecik, R. Kumar, A. Maj, S. Mandal, F. Montes, S. Myalski, G. S. Simpson, S. J. Steer, S. Tashenov, and O. Wieland, *Phys. Rev. Lett.* **99**, 132501 (2007).
- [56] S. Ilieva, M. Thürauf, Th. Kröll, R. Krücken, T. Behrens, V. Bildstein, A. Blazhev, S. Bönig, P. A. Butler, J. Cederkäll, T. Davinson, P. Delahaye, J. Diriken, A. Ekström, F. Finke, L. M. Fraile, S. Franchoo, Ch. Fransen, G. Georgiev, R. Gernhäuser, D. Habs, H. Hess, A. M. Hurst, M. Huyse, O. Ivanov, J. Iwanicki, P. Kent, O. Kester, U. Köster, R. Lutter, M. Mahgoub, D. Martin, P. Mayet, P. Maierbeck, T. Morgan, O. Niedermeier, M. Pantea, P. Reiter, T. R. Rodríguez, Th. Rolke, H. Scheit, A. Scherillo, D. Schwalm, M. Seidlitz, T. Sieber, G. S. Simpson, I. Stefanescu, S. Thiel, P. G. Thirolf, J. Van de Walle, P. Van Duppen, D. Voulot, N. Warr, W. Weinzierl, D. Weishaar, F. Wenander, A. Wiens, and S. Winkler, *Phys. Rev. C* **89**, 014313 (2014).
- [57] T. Kautzsch, W. B. Walters, M. Hannawald, K.-L. Kratz, V. I. Mishin, V. N. Fedoseyev, W. Böhmer, Y. Jading, P. Van Duppen, B. Pfeiffer, A. Wöhr, P. Möller, I. Klöckl, V. Sebastian, U. Köster, M. Koizumi, J. Lettry, H. L. Ravn, and the ISOLDE Collaboration, *Eur. Phys. J. A* **9**, 201 (2000).
- [58] M. Danchev, G. Rainovski, N. Pietralla, A. Gargano, A. Covello, C. Baktash, J. R. Beene, C. R. Bingham, A. Galindo-Uribarri, K. A. Gladnishki, C. J. Gross, V. Yu. Ponomarev, D. C. Radford, L. L. Riedinger, M. Scheck, A. E. Stuchbery, J. Wambach, C.-H. Yu, and N. V. Zamfir, *Phys. Rev. C* **84**, 061306(R) (2011).
- [59] R. L. Varner, J. R. Beene, C. Baktash, A. Galindo-Uribarri, C. J. Gross, J. Gomez del Campo, M. L. Halbert, P. A. Hausladen, Y. Larochele, J. F. Liang, J. Mas, P. E. Mueller, E. Padilla-Rodal, D. C. Radford, D. Shapira, D. W. Stracener, J.-P. Urrego-Blanco, and C.-H. Yu, *Eur. Phys. J. A* **25**, 391 (2005).
- [60] H. Watanabe, G. Lorusso, S. Nishimura, Z. Y. Xu, T. Sumikama, P.-A. Söderström, P. Doornenbal, F. Browne, G. Gey, H. S. Jung, J. Taprogge, Zs. Vajta, J. Wu, A. Yagi, H. Baba, G. Benzoni, K. Y. Chae, F. C. L. Crespi, N. Fukuda, R. Gernhäuser, N. Inabe, T. Isobe, A. Jungclaus, D. Kameda, G. D. Kim, Y. K. Kim, I. Kojouharov, F. G. Kondev, T. Kubo, N. Kurz, Y. K. Kwon, G. J. Lane, Z. Li, C.-B. Moon, A. Montaner-Pizá, K. Moschner, F. Naqvi, M. Niikura, H. Nishibata, D. Nishimura, A. Odahara, R. Orlandi, Z. Patel, Zs. Podolyák, H. Sakurai, H. Schaffner, G. S. Simpson, K. Steiger, H. Suzuki, H. Takeda, A. Wendt, and K. Yoshinaga, *Phys. Rev. Lett.* **111**, 152501 (2013).
- [61] H. Mach, D. Jerrestam, B. Fogelberg, M. Hellström, J.

- P. Omtvedt, K. I. Erokhina, and V. I. Isakov, Phys. Rev. C **51**, 500 (1995).
- [62] J. J. Cuenca-García, G. Martínez-Pinedo, K. Langanke, F. Nowacki, and I. N. Borzov, F. Montes, Eur. Phys. J. A **34**, 99 (2007).
- [63] I. N. Borzov, *Fission and Properties of Neutron-Rich Nuclei*, edited by J. H. Hamilton, A. V. Ramayya (World Scientific, Singapore, 2014), p. 530.